

MĂDĂLINA DUMITRIU¹, CĂTĂLIN CRUCEANU¹

INFLUENCES OF CARBODY VERTICAL FLEXIBILITY ON RIDE COMFORT OF RAILWAY VEHICLES

The article investigates the influence of the carbody vertical flexibility on the ride comfort of the railway vehicles. The ride comfort is evaluated via the comfort index calculated in three reference points of the carbody. The results of the numerical simulations bring attention to the importance of the carbody symmetrical vertical bending upon the dynamic response of the vehicle, mainly at high velocities. Another conclusion is that the ride comfort can be significantly affected as a function of the symmetrical bending frequency of the carbody. Similarly, there are improvement possibilities for the ride comfort when the best selection of the stiffness in the longitudinal traction system between the carbody and bogie and the vertical suspension damping is made.

1. Introduction

During running, the railway vehicle is subjected to a constant regime of vertical vibrations, with negative effects on the ride quality, ride comfort and safety. The vertical vibrations mainly derive from the vehicle running on a track with vertical irregularities. Such vibrations comprise the simple vibration modes of the vehicle suspended masses – the rigid modes (bound, pitch and rebound), to which the complex vibration modes are added (structural vibrations), global or local, due to the carbody flexibility, namely the bending and torsion, the modes of diagonal torsion and the local deformations of the floor, walls or ceiling [1].

For high speed vehicles, a large number of theoretical and experimental studies have confirmed that the level of vibrations can be strongly affected by the resonance phenomenon of the vibration flexible modes in the carbody[2–6]. Even though the carbody structural vibrations are rather complex [7, 8], the greatest influence on comfort during vibrations comes from the first carbody natural bending mode

¹Department of Railway Vehicles, University Politehnica of Bucharest, Bucharest, Romania.
Emails: madalinadumitriu@yahoo.com, c_cruceanu@yahoo.com

(symmetrical bending) whose frequency usually ranges from 6 to 12 Hz [3], an interval where the human body shows a higher sensitivity to vertical vibrations.

The carbody structural vibrations generally occur in the vehicle of a light structure, such as the ones meant for passenger transport, where this solution was adopted to maximize usage of the limited axle loads. But the light weight design, while satisfying the requirements of strength and crashworthiness, is achieved usually at a cost of significant decrease in structural stiffness, and consequently the decrease of bending frequencies [2]. A lower structural stiffness in the carbody triggers a worse ride comfort, mainly at the carbody centre; in some cases, repositioning of the critical points in terms of comfort will take place, from the carbody ends to its centre [9].

This article investigates the influence of the carbody vertical flexibility on the ride comfort during the carbody running on a track with vertical irregularities. The investigation process involves a model of the vehicle often mentioned in the literature [2, 5] including a “flexible carbody” model that considers the rigid vibration modes – bounce and pitch and its first flexible vibration mode – the symmetrical vertical bending and six rigid bodies that represent the axles and the suspended masses of the bogies. While the previous studies consider only the vertical stiffness of the secondary suspension, this paper describes the model of the secondary suspension including important elements – the pitch stiffness and the stiffness of the longitudinal traction system between the carbody and the bogie, whereby the bogies pitch vibration is transmitted to the carbody and excites the symmetrical bending modes.

The ride comfort evaluation is based on the comfort index [10, 11], calculated in three carbody reference points – at its centre and above the two bogies, depending on the carbody vertical bending frequency. The influence of the stiffness in the longitudinal traction system between the carbody and bogie and the damping ratio of the two suspension levels on the ride comfort will be looked at and the possibilities to improve the ride comfort at high velocities will be identified.

2. The vehicle mechanical model

To study the influence of the carbody flexibility on the ride comfort, a four-axle and two-level suspension vehicle is considered, travelling at a constant velocity V on a perfectly rigid track, with vertical irregularities. The track irregularities are described with the reference to each axle by functions $\eta_{j,(j+1)}$, with $j = 2i - 1$, for $i = 1, 2$, while mentioning that each bogie is equipped with the axles j and $j + 1$.

The vehicle model (Fig. 1) includes a body with distributed parameters for the carbody and many rigid bodies for the two bogies (the suspended masses) and the four axles. These bodies are connected among them via Kelvin-Voigt type systems, which helps modelling the suspension levels.

The carbody is represented by a free-free equivalent beam, with constant section and mass uniformly distributed, of Euler-Bernoulli type. The beam parameters

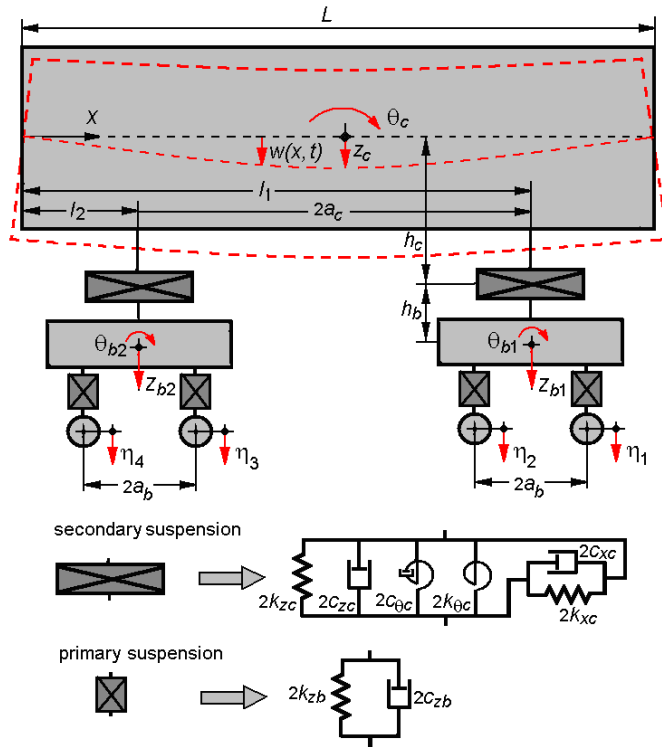


Fig. 1. The vehicle mechanical model

are defined in terms of the carbody', such as: L – beam length; $\rho_c = m_c/L$ – beam mass per length unit, where m_c is the carbody mass; μ – structural damping coefficient; EI – bending modulus, where E is the longitudinal modulus of elasticity, and I is the area moment of inertia of the beam transversal section.

There will be taken into account the carbody rigid vibration modes – bounce z_c and pitch θ_c , and the first carbody natural bending mode in a vertical plan – symmetrical bending. The carbody inertia reported to the rigid vibration modes is represented by mass m_c and the mass moment of inertia J_c .

The carbody movement $w(x,t)$ comes from the superposition of the rigid vibration modes with the first bending mode

$$w(x,t) = z_c(t) + \left(x - \frac{L}{2}\right) \theta_c(t) + X_c(x)T_c(t), \quad (1)$$

where $T_c(t)$ is the coordinate of the first natural bending mode in a vertical plan and $X_c(x)$ stands for its eigenfunction

$$X_c(x) = \sin \beta x + \sinh \beta x - \frac{\sin \beta L - \sinh \beta L}{\cos \beta L - \cosh \beta L} (\cos \beta x + \cosh \beta x) \quad (2)$$

with

$$\beta = \sqrt[4]{\omega_c^2 \rho_c / (EI)} \quad (3)$$

and

$$\cos \beta L \cosh \beta L - 1 = 0, \quad (4)$$

where ω_c is the natural angular frequency of the symmetrical bending in the carbody.

The bogies have two degrees of freedom: bounce z_{bi} and pitch θ_{bi} , with $i = 1, 2$. Each bogie has the mass m_b and mass moment of inertia J_b . The bogie wheelbase is $2a_b$, and the distance between the bogies' axles is $2a_c$.

To represent the suspension components of the railway vehicles, both relatively simple linear and more sophisticated models, nonlinear and load-sensitive models and frequency-dependent models can be chosen; multi-physics models may also be included, for instance, in the case of air springs suspension and active components. However, the modeling of suspension requires good judgement to be successful. In most cases, the complex models for the suspension are difficult to handle and require too much computing time when implemented in the numerical simulation codes of vehicle dynamics. Qualitative and even quantitative information may be obtained by using even less complex models. The level of details in modelling the suspension depends on the purpose of the analysis [12]. Herein, the objective of the work is centred on the influence of the carbody vertical flexibility on the ride comfort; hence, the simpler model of Kelvin-Voigt has been adopted, usually found in such studies [2, 13, 14]. The Kelvin-Voigt model can be even applied to represent the air spring suspension in the vertical direction, a suspension which fits the typical modern passenger vehicles [12].

The modelling of the secondary suspension of a bogie is done via two Kelvin-Voigt, one for vertical translation and another for rotation, with the vertical stiffness $2k_{zc}$ and the pitch angular stiffness $2k_{\theta c}$, as well as the damping constants are $2c_{zc}$ and $2c_{\theta c}$. The Kelvin-Voigt system positioned in the vertical direction at distance h_c from the carbody's neutral axis and at distance h_b from the bogie centre of gravity models the longitudinal traction system between the carbody and the bogie. This has the elastic constant $2k_{xc}$ and the damping constant $2c_{xc}$.

The primary suspension corresponding to an axle is modelled by a Kelvin-Voigt system operating on translation in the vertical direction, with the elastic constant $2k_{zb}$, and the damping constant $2c_{zb}$.

3. Movement equations

The carbody vertical motions are described by the equations of the rigid vibration modes of the carbody and of the bogies – bounce and pitch, as well as by the equation of the first natural bending mode of the carbody – symmetrical bending.

The equation of motion for the carbody has the form of

$$EI \frac{\partial^4 w(x, t)}{\partial x^4} + \mu I \frac{\partial^5 w(x, t)}{\partial x^4 \partial t} + \rho_c \frac{\partial^2 w(x, t)}{\partial t^2} = \sum_{i=1}^2 F_{zci} \delta(x - l_i) - \sum_{i=1}^2 (M_{ci} - h_c F_{xci}) \frac{d\delta(x - l_i)}{dx}, \quad (5)$$

where $\delta(\cdot)$ is the Dirac's delta function, the distances l_i set the position of the carbody supporting points on the secondary suspension and F_{xci} , F_{zci} and M_{ci} stand for the forces, respectively the moments derived from the secondary suspension of the bogie i

$$F_{zci} = -2c_{zc} \left(\frac{\partial w(l_i, t)}{\partial t} - \dot{z}_{bi} \right) - 2k_{zc} [w(l_i, t) - z_{bi}]; \quad (6)$$

$$F_{xci} = 2c_{xc} \left(h_c \frac{\partial^2 w(l_i, t)}{\partial x \partial t} + h_b \dot{\theta}_{bi} \right) + 2k_{xc} \left(h_c \frac{\partial w(l_i, t)}{\partial x} + h_b \theta_{bi} \right); \quad (7)$$

$$M_{ci} = -2c_{\theta c} \left(\frac{\partial^2 w(l_i, t)}{\partial x \partial t} - \dot{\theta}_{bi} \right) - 2k_{\theta c} \left[\frac{\partial w(l_i, t)}{\partial x} - \theta_{bi} \right]. \quad (8)$$

Upon the application of the modal analysis method and considering the orthogonality property of the eigenfunctions of the carbody bending modes, the equation of motion (5) is changed into three second-order differential equations with ordinary derivatives that describe the bounce, pitch and symmetrical bending carbody motions:

$$m_c \ddot{z}_c = \sum_{i=1}^2 F_{zci}; \quad (9)$$

$$J_c \ddot{\theta}_c = \sum_{i=1}^2 F_{zci} \left(l_i - \frac{L}{2} \right) + \sum_{i=1}^2 (M_{ci} - h_c F_{xci}); \quad (10)$$

$$m_{mc} \ddot{T}_c + c_{mc} \dot{T}_c + k_{mc} T_c = \sum_{i=1}^2 F_{zci} X_c(l_i) + \sum_{i=1}^2 (M_{ci} - h_c F_{xci}) \frac{dX_c(l_i)}{dx}, \quad (11)$$

where the carbody stiffness, damping and modal mass are given in the below relations

$$k_{mc} = EI \int_0^L \left(\frac{d^2 X_c}{dx^2} \right) dx; \quad c_{mc} = \mu I \int_0^L \left(\frac{d^2 X_c}{dx^2} \right) dx; \quad (12)$$

$$m_{mc} = \rho_c \int_0^L X_c^2 dx.$$

If equations (7)–(9) are replaced in the carbody movement equations and based on the symmetry properties of the eigenfunction $X_c(x)$, the following notations are introduced

$$X_c(l_1) = X_c(l_2) = \varepsilon; \quad (13)$$

$$\frac{dX_c(l_1)}{dx} = -\frac{dX_c(l_2)}{dx} = \lambda, \quad (14)$$

and hence written:

$$m_c \ddot{z}_c + 2c_{zc} [2\dot{z}_c + 2\varepsilon \dot{T}_c - (\dot{z}_{b1} + \dot{z}_{b2})] + 2k_{zc} [2z_c + 2\varepsilon T_c - (z_{b1} + z_{b2})] = 0; \quad (15)$$

$$\begin{aligned} J_c \ddot{\theta}_c + 2c_{zc} a_c [2a_c \dot{\theta}_c - (\dot{z}_{b1} - \dot{z}_{b2})] + 2k_{zc} a_c [2a_c \theta_c - (z_{b1} - z_{b2})] + \\ + 2c_{xc} h_c [2h_c \dot{\theta}_c + h_b (\dot{\theta}_{b1} + \dot{\theta}_{b2})] + 2k_{xc} h_c [2h_c (\theta_{b1} + \theta_{b2})] + \\ + 2c_{\theta c} [2\dot{\theta}_c - (\dot{\theta}_{b1} + \dot{\theta}_{b2})] + 2k_{\theta c} [2\theta_c - (\theta_{b1} + \theta_{b2})] = 0; \end{aligned} \quad (16)$$

$$\begin{aligned} m_{mc} \ddot{T}_c + c_{mc} \dot{T}_c + k_{mc} T_c + \\ + 2c_{zc} \varepsilon [2\dot{z}_c + 2\varepsilon \dot{T}_c - (\dot{z}_{b1} + \dot{z}_{b2})] + 2k_{zc} \varepsilon [2z_c + 2\varepsilon T_c - (z_{b1} + z_{b2})] + \\ + 2c_{xc} h_c \lambda [2h_c \lambda \dot{T}_c + h_b (\dot{\theta}_{b1} - \dot{\theta}_{b2})] + 2k_{xc} h_c \lambda [2h_c \lambda T_c + h_{b2} (\theta_{b1} - \theta_{b2})] + \\ + 2c_{\theta c} \lambda [2\lambda \dot{T}_c - (\dot{\theta}_{b1} - \dot{\theta}_{b2})] + 2k_{\theta c} \lambda [2\lambda T_c - (\theta_{b1} - \theta_{b2})] = 0. \end{aligned} \quad (17)$$

The equations describing the bounce and pitch motions of the bogies are:

$$m_b \ddot{z}_{bi} = \sum_{j=2i-1}^{2i} F_{zbj, (j+1)} - F_{zci}, \quad \text{with } i = 1, 2; \quad (18)$$

$$J_b \ddot{\theta}_{bi} = a_b \sum_{j=2i-1}^{2i} (-1)^{j+1} F_{zbj} - M_{ci} - h_b F_{xci}, \quad \text{with } i = 1, 2, \quad (19)$$

where $F_{zbj, j+1}$ represent the forces due to the primary suspension corresponding to the axles j and $(j + 1)$, respectively

$$F_{zbj, (j+1)} = -2c_{zb} (\dot{z}_{bi} \pm a_b \dot{\theta}_{bi} - \dot{\eta}_{j, (j+1)}) - 2k_{zb} (z_{bi} \pm a_b \theta_{bi} - \eta_{j, (j+1)}). \quad (20)$$

After processing, the equations (18) and (19) are as such:

$$\begin{aligned} m_b \ddot{z}_{bi} + 2c_{zb} [2\dot{z}_{bi} - (\dot{\eta}_j + \dot{\eta}_{(j+1)})] + 2k_{zb} [2z_{bi} - (\eta_j + \eta_{(j+1)})] \\ + 2c_{zc} (\dot{z}_{bi} - \dot{z}_c \mp a_c \dot{\theta}_c - \varepsilon \dot{T}_c) + 2k_{zc} (z_{bi} - z_c \mp a_c \theta_c - \varepsilon T_c) = 0; \end{aligned} \quad (21)$$

$$\begin{aligned}
 & J_b \ddot{\theta}_{bi} + 2c_{zb} a_b [2a_b \dot{\theta}_{bi} - (\dot{\eta}_j - \dot{\eta}_{(j+1)})] + 2k_{zb} a_b [2a_b \theta_{bi} - (\eta_j - \eta_{(j+1)})] + \\
 & + 2c_{xc} h_b [h_b \dot{\theta}_{bi} + h_c (\dot{\theta}_c \pm \lambda \dot{T}_c)] + 2k_{xc} h_b [h_b \theta_{bi} + h_c (\theta_c \pm \lambda T_c)] + \\
 & + 2c_{\theta c} (\dot{\theta}_{bi} - \dot{\theta}_c \mp \lambda \dot{T}_c) + 2k_{\theta c} (\theta_{bi} - \theta_c \mp \lambda T_c) = 0.
 \end{aligned} \quad (22)$$

The system including the equations (15)-(17) and (21)-(22) will be matrix-like written:

$$\mathbf{M}\ddot{\mathbf{p}} + \mathbf{C}\dot{\mathbf{p}} + \mathbf{K}\mathbf{p} = \mathbf{P}\dot{\boldsymbol{\eta}} + \mathbf{R}\boldsymbol{\eta}, \quad (23)$$

where \mathbf{M} , \mathbf{C} and \mathbf{K} are the inertia, damping and stiffness matrices, respectively, and \mathbf{P} and \mathbf{R} are the track displacement and velocity input matrices.

4. The steady-state harmonic regime of vibration. The frequency response functions

This section features the steady-state harmonic behaviour, with the purpose to calculate the frequency response functions of the vehicle. In the next section, these functions will help with the calculation of the frequency response function of the vehicle corresponding to random behaviour of vibrations in the form of the spectral power density of the acceleration.

It is considered that the track vertical irregularities are in a harmonic shape with the wavelength Λ and amplitude η_0 . With the reference to each axle, the vertical irregularities of the track can be written as

$$\eta_{1,2}(x) = \eta_0 \cos \frac{2\pi}{\Lambda} (x + a_c \pm a_b); \quad \eta_{3,4}(x) = \eta_0 \cos \frac{2\pi}{\Lambda} (x - a_c \pm a_b), \quad (24)$$

where $x = Vt$ is the coordinate of the carbody centre. The functions $\eta_{j,j+1}$, with $j = 2i - 1$ for $i = 1, 2$, can be expressed as time harmonic functions

$$\eta_{1,2}(t) = \eta_0 \cos \omega \left(t + \frac{a_c \pm a_b}{V} \right); \quad \eta_{3,4}(t) = \eta_0 \cos \omega \left(t - \frac{a_c \mp a_b}{V} \right), \quad (25)$$

in which $\omega = 2\pi V/\Lambda$ means the angular frequency induced by the track excitation.

As for the vehicle response, this is assumed to be harmonic, with the same frequency as the track excitation induced frequency. The coordinates describing the motions of the vehicle are written under the general form as

$$p_k(t) = P_k \cos(\omega t + \varphi_k), \quad \text{with } k = 1 \div 7, \quad (26)$$

where P_k is the amplitude, and φ_k represents the phase of the coordinate k compared to the track vertical irregularities with respect to the vehicle centre.

In addition, the complex values associated with the real ones, for $i^2 = -1$:

$$\bar{\eta}_{j,j+1}(t) = \bar{\eta}_{j,j+1} e^{i\omega t}, \quad \text{for } j = 2i - 1 \quad \text{and } i = 1, 2; \quad (27)$$

$$\bar{p}_k(t) = \bar{P}_k e^{i\omega t}, \quad (28)$$

in the system of equations (23). A linear system of algebraic heterogeneous equations is obtained

$$(-\omega^2 \mathbf{M} + \mathbf{A}) \bar{\mathbf{P}} = \eta_0 \mathbf{B}, \quad (29)$$

where:

$$\bar{\mathbf{P}} = \bar{\mathbf{P}}(\omega) = [\bar{P}_1 \ \bar{P}_2 \ \dots \ \bar{P}_7]^T;$$

$$\mathbf{M} = \text{diag}(m_c \ J_c \ m_{mc} \ m_b \ J_b \ m_b \ J_b);$$

$$\mathbf{A} = \begin{bmatrix} 2\alpha_{zc} & 0 & 2\varepsilon\alpha_{zc} & -\alpha_{zc} & 0 & -\alpha_{zc} & 0 \\ 0 & A_1 & 0 & -a_c\alpha_{zc} & A_3 & -a_c\alpha_{zc} & A_3 \\ 2\varepsilon\alpha_{zc} & A_2 & 0 & -\varepsilon\alpha_{zc} & \lambda C_3 & -\varepsilon\alpha_{zc} & -\lambda A_3 \\ -\alpha_{zc} & -a_c\alpha_{zc} & \varepsilon\alpha_{zc} & 2\alpha_{zb} + \alpha_{zc} & 0 & 0 & 0 \\ 0 & A_3 & \lambda A_3 & 0 & A_4 & 0 & 0 \\ -\alpha_{zc} & a_c\alpha_{zc} & \varepsilon\alpha_{zc} & 0 & 0 & 2\alpha_{zb} + \alpha_{zc} & 0 \\ 0 & A_3 & -\lambda A_3 & 0 & 0 & 0 & A_4 \end{bmatrix},$$

where the notations below have been introduced

$$\alpha_{zc} = 2(i\omega c_{zc} + k_{zc}); \quad \alpha_{xc} = 2(i\omega c_{xc} + k_{xc});$$

$$\alpha_{\theta c} = 2(i\omega \theta_c + k_{\theta c}); \quad \alpha_{mc} = i\omega c_{mc} + k_{mc}; \quad \alpha_{zb} = 2(i\omega c_{zb} + k_{zb});$$

$$A_1 = 2a_c^2\alpha_{zc} + 2h_c^2\alpha_{xc} + 2\alpha_{\theta c}; \quad A_2 = \alpha_{mc} + 2\varepsilon^2\alpha_{zc} + 2h_c^2\lambda^2\alpha_{xc} + 2\lambda^2\alpha_{\theta c};$$

$$A_3 = h_c h_b \alpha_{xc} - \alpha_{\theta c}; \quad A_4 = 2a_b^2\alpha_{zb} + h_b^2\alpha_{xc} = \alpha_{\theta c};$$

$$\mathbf{B} = 2\alpha_{zb} \begin{bmatrix} 0 \\ 0 \\ 0 \\ \exp(i\omega a_c/V) \cos(\omega a_b/V) \\ ia_b \exp(i\omega a_c/V) \sin(\omega a_b/V) \\ \exp(-i\omega a_c/V) \cos(\omega a_b/V) \\ ia_b \exp(-i\omega a_c/V) \sin(\omega a_b/V) \end{bmatrix}.$$

When the system of equations (29) is solved, the frequency response functions of the vehicle can be determined. The response function of the carbody movement

in a certain point x situated on the carbody longitudinal axis that goes through its mass centre is as follows

$$\bar{H}_c(x, \omega) = \bar{H}_{z_c}(\omega) + \left(\frac{L}{2} - x\right) \bar{H}_{\theta_c}(\omega) + X_c(x) \bar{H}_{T_c}(\omega), \quad (30)$$

where $\bar{H}_{z_c}(\omega)$, $\bar{H}_{\theta_c}(\omega)$, $\bar{H}_{T_c}(\omega)$ are the response functions corresponding to the rigid vibration modes, bounce and pitch (z_c and θ_c), and to the first natural vertical bending mode of the carbody (T_c)

$$\bar{H}_{z_c}(\omega) = \frac{\bar{P}_1(\omega)}{\bar{\eta}_0}; \quad \bar{H}_{\theta_c}(\omega) = \frac{\bar{P}_2(\omega)}{\bar{\eta}_0}; \quad \bar{H}_{T_c}(\omega) = \frac{\bar{P}_3(\omega)}{\bar{\eta}_0}. \quad (31)$$

The response function of the carbody acceleration can be calculated as depending on the vertical displacement

$$\bar{H}_{ac}(x, \omega) = \omega^2 \bar{H}_c(x, \omega). \quad (32)$$

The relation (32) can be customized for various points along the carbody. The acceleration response function at the carbody centre is thus

$$\bar{H}_{acm}(\omega) = \omega^2 \bar{H}_c\left(\frac{L}{2}, \omega\right) = \omega^2 \left[\bar{H}_{z_c}(\omega) + \left(\frac{L}{2}\right) \bar{H}_{T_c}(\omega) \right], \quad (33)$$

and above the two bogies

$$\bar{H}_{acbi}(\omega) = \omega^2 \bar{H}_c(l_i, \omega) = \omega^2 \left[\bar{H}_{z_c}(\omega) \pm a_c \bar{H}_{\theta_c}(\omega) + X_c(l_i) \bar{H}_{T_c}(\omega) \right]. \quad (34)$$

for $i = 1, 2$.

5. The regime of the stochastic vibrations

The track vertical irregularities are considered to represent a stationary stochastic process that can be described by means of the power spectral density. The theoretical curve of the power spectral density is representative for the average statistical properties of the European railway, as in the relation [15]

$$S(\Omega) = \frac{A\Omega_c^2}{(\Omega^2 + \Omega_r^2)(\Omega^2 + \Omega_c^2)}, \quad (35)$$

where Ω is the wavelength, $\Omega_c = 0.8246$ rad/m, $\Omega_r = 0.0206$ rad/m, and A is a coefficient depending on the track quality. For a high level quality track, $A = 4.032 \cdot 10^{-7}$ rad m, whereas for a low level quality, the coefficient A is $1.080 \cdot 10^{-6}$ rad m.

As a function of the angular frequency $\omega = V\Omega$, the power spectral density of the track irregularities can be written as in the general relation

$$G(\omega) = \frac{S(\omega/V)}{V}. \quad (36)$$

What results is the power spectral density of the track irregularities in the form of

$$G(\omega) = \frac{A\Omega_c^2 V^3}{[\omega^2 + (V\Omega_c)^2][\omega^2 + (V\Omega_r)^2]}. \quad (37)$$

Starting from the response function of the carbody acceleration in equation (32) and from the spectrum of the track irregularities in equation (37), power spectral density of the carbody vertical acceleration can be determined, as per the relation below

$$G_{ac}(x, \omega) = G(\omega) |\overline{H}_{ac}(x, \omega)|^2. \quad (38)$$

When customizing the relation (38), the power spectral density of the acceleration in the reference point at the carbody centre and above the bogies will be as follows:

$$G_{acm}(\omega) = G(\omega) |\overline{H}_{acm}(\omega)|^2; \quad (39)$$

$$G_{acb_{1,2}}(\omega) = G(\omega) |\overline{H}_{acb_{1,2}}(\omega)|^2. \quad (40)$$

Further on, the root mean square acceleration in a random carbody point can be calculated based on the vehicle dynamic response expressed as the power spectral density of the carbody acceleration

$$a(x) = \sqrt{\frac{1}{\pi} \int_0^\infty G_{ac}(x, \omega) d\omega}, \quad (41)$$

or in its reference points:

– at the carbody centre

$$a_m = \sqrt{\frac{1}{\pi} \int_0^\infty G_{cam}(\omega) d\omega}; \quad (42)$$

– above the two bogies

$$a_{b_{1,2}} = \sqrt{\frac{1}{\pi} \int_0^\infty G_{acb_{1,2}}(\omega) d\omega}. \quad (43)$$

It should be mentioned that the root mean square acceleration is useful for calculating the comfort index, as seen in the next section.

6. Comfort index-based evaluation of the ride comfort

To quantify the comfort to vibrations, a parameter is needed, i.e. the comfort index, and a scale to connect the values of this parameter and the comfort feeling (Table 1). Thus, a conventional scale of the comfort index has been set up [10, 11].

Table 1.

The significance of the comfort index

| Comfort index N_M | Significance |
|---------------------|--------------------|
| $N_M < 1$ | very good comfort |
| $1 \leq N_M < 2$ | good comfort |
| $2 \leq N_M < 4$ | acceptable comfort |
| $4 \leq N_M < 5$ | poor comfort |
| $N_M \geq 5$ | very poor comfort |

To evaluate the comfort in the vertical direction, the partial comfort index is used, which is calculated with the relation [10]

$$N_{MV} = 6a_{95}^{W_{ab}}, \quad (44)$$

where a is the root mean square of the vertical acceleration, 95 refers to the quantile of order 95%, and $W_{ab} = W_a W_b$ represents the weighting filter of the accelerations in the vertical direction [11]. The filter W_a is a band-pass type filter, with the following transfer function

$$H_a(s) = \frac{s^2(2\pi f_2)^2}{\left[s^2 + \frac{2\pi f_1}{Q_1} s + (2\pi f_1)^2 \right] \left[s^2 + \frac{2\pi f_2}{Q_1} s + (2\pi f_2)^2 \right]}, \quad (45)$$

with $f_1 = 0.4$ Hz, $f_2 = 100$ Hz and $Q_1 = 0.71$.

The weighting filter W_b , which takes into account the higher human sensitivity to the vertical vibrations within the frequencies ranging from 3 to 13 Hz, has the transfer function in the form of

$$H_a(s) = \frac{(s + 2\pi f_3) \left[s^2 + \frac{2\pi f_5}{Q_3} s + (2\pi f_5)^2 \right] 2\pi K f_4^2 f_6^2}{\left[s^2 + \frac{2\pi f_4}{Q_2} s + (2\pi f_4)^2 \right] \left[s^2 + \frac{2\pi f_6}{Q_4} s + (2\pi f_6)^2 \right] f_3 f_5^2}, \quad (46)$$

where $f_3 = 16$ Hz, $f_4 = 16$ Hz, $f_5 = 2.5$ Hz, $f_6 = 4$ Hz, $Q_2 = 0.63$, $Q_4 = 0.8$, $K = 0.4$ and $s = i\omega$.

When adopting the hypothesis that the vertical accelerations have a Gaussian distribution with the null mean value and considering the relation (41) to calculate

the root mean square acceleration, the following relation for the comfort index is derived

$$N_{MV}(x) = 6\Phi^{-1}(0.95) \sqrt{\frac{1}{\pi} \int_0^{\infty} G_{ac}(x, \omega) |H_{ab}(\omega)|^2 d\omega}, \quad (47)$$

where $\Phi^{-1}(0.95)$ represents the quantile of the standard Gaussian distribution with the probability of 95% and $H_{ab}(\omega) = H_a(\omega)H_b(\omega)$.

To calculate the comfort index in the carbody reference points, namely at the centre and above the bogies, the particular relations (39)–(40) of the acceleration power spectral density are considered.

7. Numerical application

The numerical simulations pertinent to the influence of the carbody bending upon the ride comfort are presented below, derived from the model and the evaluation method of comfort shown in the previous sections.

The parameters of the vehicle used in the numerical simulations are introduced in the Table 2. The natural frequencies of the vibration rigid modes in the carbody and bogies and the carbody bending frequency, corresponding to the parameters in Table 2, are featured in Table 3. They have typical values for a high speed passenger vehicle [16].

Table 2.

The parameters of the vehicle numerical model

| | |
|---|-----------------------------|
| $m_c = 34.0 \cdot 10^3$ kg | $2k_{zc} = 1.20$ MN/m |
| $m_b = 3.20 \cdot 10^3$ kg | $2k_{xc} = 4.00$ MN/m |
| $J_c = 1.96 \cdot 10^6$ kg·m ² | $2k_{\theta c} = 256$ kN/m |
| $J_b = 2.05 \cdot 10^3$ kg·m ² | $2c_{zc} = 34.3$ kN·s/m |
| $EI = 3.16 \cdot 10^9$ N·m ² | $2c_{xc} = 50.0$ kN·s/m |
| $m_{mc} = 35.2 \cdot 10^3$ kg | $2c_{\theta c} = 2.00$ kN·m |
| $L = 26.4$ m | $k_{mc} = 89.0$ MN/m |
| $2a_c = 19.0$ m; $2a_b = 2.56$ m | $c_{mc} = 53.1$ kN·m/s |
| $h_c = 1.30$ m | $4k_{zb} = 4.40$ MN/m |
| $h_b = 0.20$ m | $4c_{zb} = 52.2$ kN·s/m |

When considering the vehicle parameters in Table 2, the power spectral density of the vertical acceleration will be calculated in the carbody reference points – at the centre and above the two bogies for velocities of up to 300 km/h (see Fig. 2).

What can be noticed at the carbody centre is that the power spectral density of the acceleration is dominated by the carbody bounce at 1.17 Hz. In the reference points above the two bogies, the carbody bounce and pitch are dominant (1.46 Hz). Similarly, the peaks corresponding to the carbody bending at 8 Hz can be viewed

Table 3.

The natural frequencies of the vehicle vibration modes

| Vibration mode | Frequency |
|-----------------|-----------|
| Carbody bounce | 1.17 Hz |
| Carbody pitch | 1.46 Hz |
| Carbody bending | 8.00 Hz |
| Bogie bounce | 6.61 Hz |
| Bogie pitch | 9.63 Hz |

in all the reference points, but this vibration mode has a higher percentage at the carbody centre, mainly for high velocities. Besides the peaks for the resonance frequencies of the carbody vibration modes, there is a series of minimum values corresponding to the geometric filtering effect.

The geometric filtering effect is an essential feature of the behaviour of vertical vibrations in the railway vehicles, extensively analysed in many papers [2, 5, 6, 17–21]. This effect is mainly due to the manner in which the track excitations are conveyed to the suspended masses via the axles, irrespective of the suspension characteristics. Essentially, the geometric filtering effect is the result of the displacement between the vertical movements in the axles coming from running on a track with irregularities; this displacement derives from the axle position in the assembly of the running gear and the vehicle velocity. This fact gives the geometric filtering a selective nature, depending on the vehicle wheelbases and velocity and on a differentiated efficiency, along the vehicle carbody and the movement behavior, respectively [21].

When running over the track irregularities and due to the geometric filtering effect, the vehicle response would include a succession of maximum and minimum points, depending on the distance between the axles and on velocity. The maximum points correspond to the situation where the geometric filtering does not operate, while the minimum points show themselves as anti-resonance frequencies that are consistent with the geometric filtering frequencies. Should the anti-resonance frequencies coincide with the natural frequency of one of the vehicle's natural vibration modes, then its influence is much diminished. This is how the change of the importance of the natural vibration modes in the vehicle can be explained in dependence on the velocity while stating the fact that the vibrations' behaviour does not continuously intensify when velocity increases [6].

Fig. 3 shows the power spectral density of the carbody vertical acceleration, weighted by the transfer function of the acceleration weighting filter ($W_{ab} = W_a W_b$). Due to the bandpass filter W_b , the carbody dynamic response at the centre is dominated by the carbody bending frequency, mainly for high velocities. Similarly, the weight of this vibration mode also becomes important in the reference points above the two bogies. For velocities beyond 200 km/h, the spectrum of the acceleration power spectral density features the increase in the weight in the bogie bounce movement (at 6.61 Hz).

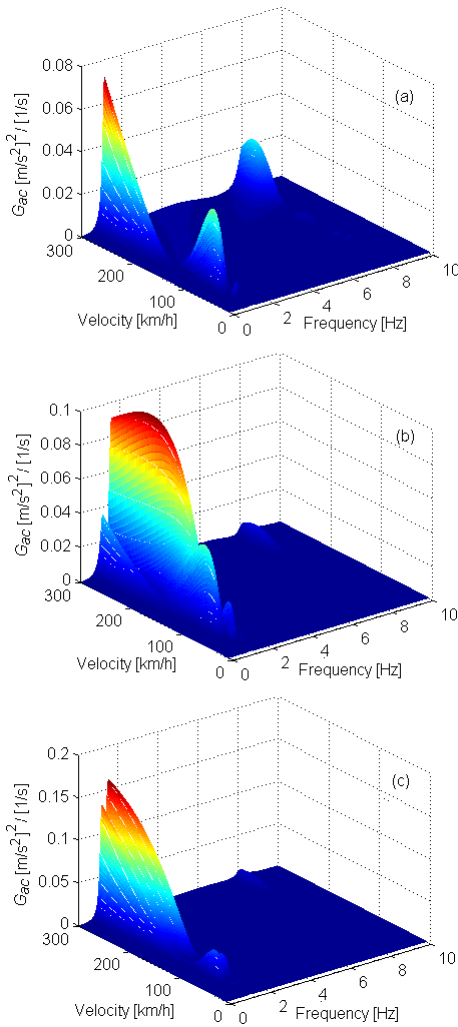


Fig. 2. Acceleration power spectral density: (a) at the carbody centre; (b) above the front bogie; (c) above the rear bogie

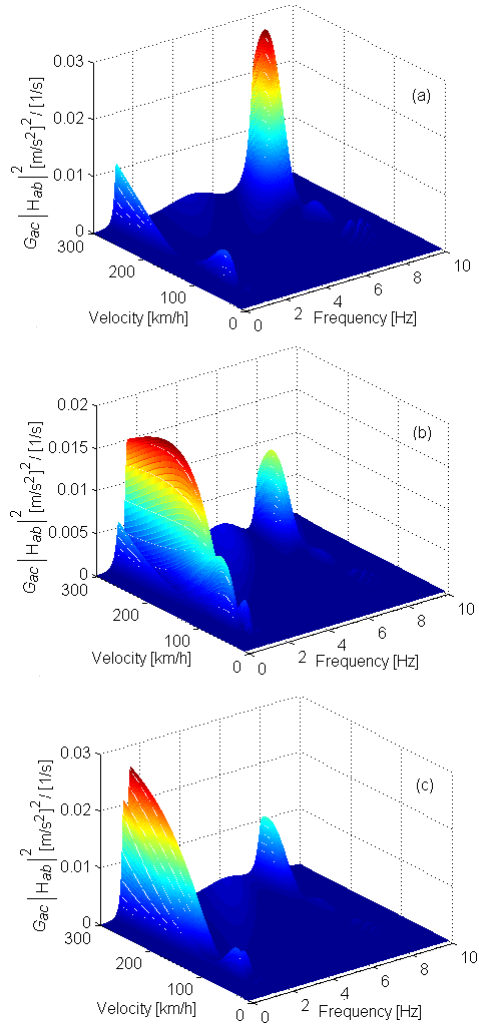


Fig. 3. Acceleration power spectral density of the weighted: (a) at the carbody centre; (b) above the front bogie; (c) above the rear bogie

Fig. 4 shows the comfort index calculated in the carbody reference points in the 150 . . . 300 km/h interval, where the carbody bending influences the dynamic response of the vehicle. Different values of the natural frequency of the carbody symmetrical bending between 6 and 14 Hz are taken into account. The diagrams confirm that the ride comfort is worse when velocity increases, essentially for carbody bending frequencies that are lower than 10 Hz. The ride comfort is better when the bending frequency rises. For instance, at 200 km/h and the bending frequency of 6 Hz, the comfort index is 2.1 at the carbody centre; 1.82 above the front bogie and 1.78 above the rear bogie. For a bending frequency of 12 Hz, the

comfort index can lower to 0.6 at the carbody centre; 1.39 above the front bogie and 1.44 above the rear bogie.

The ride comfort can be improved by an appropriate selection of the stiffness in the longitudinal traction system between the carbody and the bogie. This is shown in Fig. 5 that features the comfort index at velocity of 250 km/h, calculated in the carbody reference points for natural frequencies of its symmetrical bending ranging from 6 to 14 Hz and various values of the longitudinal stiffness k_{xc} between 0.1

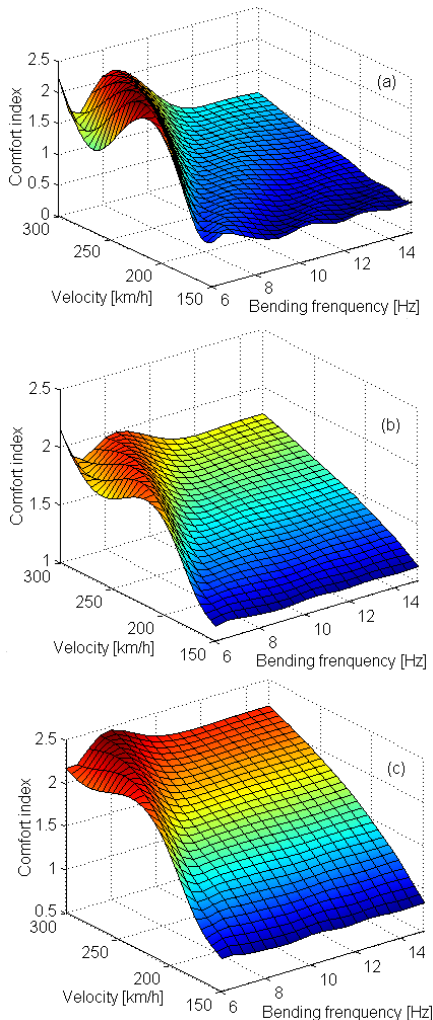


Fig. 4. The influence of the velocity upon the ride comfort: (a) at the carbody centre; (b) above the front bogie; (c) above the rear bogie

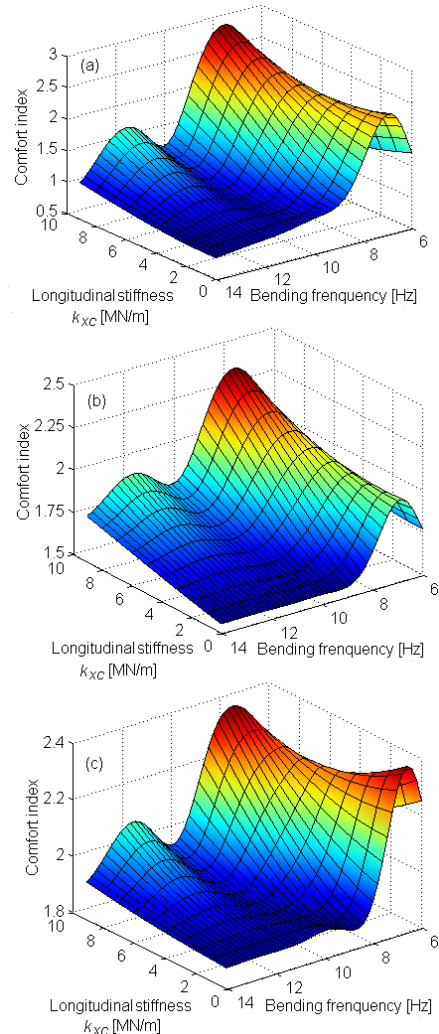


Fig. 5. The influence of the stiffness in the longitudinal traction system between the carbody and bogie upon the ride comfort: (a) at the carbody centre; (b) above the front bogie; (c) above the rear bogie

MN/m and 10 MN/m. For any of the carbody bending frequencies, the comfort index rises along with the longitudinal stiffness in the longitudinal traction system between the carbody and the bogie. For instance, Table 4 includes the values of the comfort index for the carbody bending frequency of 8 Hz.

Table 4.

The comfort index dependent on the stiffness of the longitudinal traction system between the carbody and the bogie

| k_{xc} [MN/m] | | 1 | 2 | 3 | 4 | 5 | 6 | 7 | 8 | 9 | 10 |
|-----------------|-----------------------|------|------|------|------|------|------|------|------|------|------|
| N_{MV} | at the carbody centre | 1.75 | 1.82 | 1.92 | 2.04 | 2.17 | 2.32 | 2.48 | 2.64 | 2.80 | 2.97 |
| | above the front bogie | 1.71 | 1.77 | 1.83 | 1.89 | 1.97 | 2.04 | 2.13 | 2.21 | 2.30 | 2.38 |
| | above the rear bogie | 1.94 | 1.97 | 2.00 | 2.04 | 2.08 | 2.14 | 2.19 | 2.26 | 2.32 | 2.40 |

To examine the influence of the suspension damping upon the ride comfort, the damping ratios of the suspension levels are introduced as such

$$\zeta_{zb,c} = \frac{4c_{zb,c}}{2\sqrt{4k_{zb,c}m_{b,c}}}, \quad (48)$$

that have the values of $\zeta_{zc} = 0.12$ and $\zeta_{zb} = 0.22$ for the parameters of the vehicle in Table 2.

The diagrams in Fig. 6 emphasize the influence of the damping ratio of the secondary suspension on the comfort index calculated in the carbody reference points at velocity of 250 km/h, for various values of the natural frequency of the carbody symmetrical bending. For any natural frequencies of the carbody symmetrical bending, an improvement in the ride comfort can be noticed an increase in the damping of the secondary suspension up to a certain value. An additional increase of the damping in the secondary suspension over this value will trigger the comfort deterioration. A value of the secondary suspension damping to minimize the comfort index can be identified. This value depends on the position of the carbody reference point (at the centre and above the bogies) and on the natural frequency carbody symmetrical bending, as seen in Table 5.

Table 5.

The damping ratio of the secondary suspension that minimizes the comfort index

| Bending frequency | at the carbody centre | | above the front bogie | | above the rear bogie | |
|-------------------|-----------------------|--------------|-----------------------|--------------|----------------------|--------------|
| | ζ_{zc} | N_{MV} min | ζ_{zc} | N_{MV} min | ζ_{zc} | N_{MV} min |
| 6 Hz | 0.11 | 1.53 | 0.17 | 1.72 | 0.20 | 2.08 |
| 8 Hz | 0.06 | 1.78 | 0.15 | 1.80 | 0.22 | 1.87 |
| 10 Hz | 0.13 | 0.98 | 0.19 | 1.51 | 0.26 | 1.69 |
| 12 Hz | 0.13 | 0.97 | 0.19 | 1.53 | 0.26 | 1.70 |
| 14 Hz | 0.15 | 0.84 | 0.19 | 1.52 | 0.25 | 1.69 |

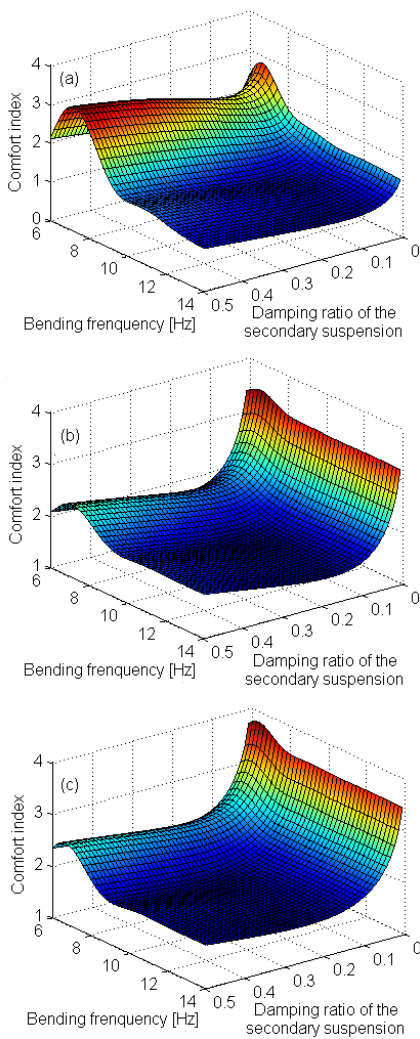


Fig. 6. The influence of the damping ratio of the secondary suspension upon the ride comfort: (a) at the carbody centre; (b) above the front bogie; (c) above the rear bogie

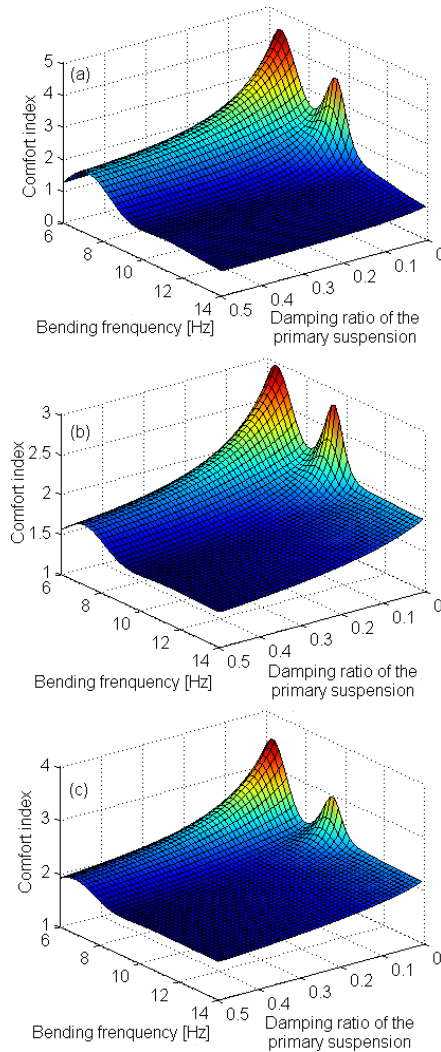


Fig. 7. The influence of the damping ratio of the primary suspension upon the ride comfort: (a) at the carbody centre; (b) above the front bogie; (c) above the rear bogie

The influence of the damping ratio of the primary suspension upon the ride comfort at velocity of 250 km/h is examined on the basis of the diagram in Fig. 7. In any of the carbody reference points, the value of the comfort index can be noticed to be lower while the damping ratio of the primary suspension is higher. This fact is included in Table 6, which features the comfort index calculated in the carbody reference points for the carbody symmetrical bending frequency of 8 Hz.

Table 6.

The comfort index depending on the damping ratio of the primary suspension

| ζ_{zb} | | 0.1 | 0.2 | 0.3 | 0.4 | 0.5 |
|--------------|-----------------------|------|------|------|------|------|
| | at the carbody centre | 2.22 | 1.95 | 1.80 | 1.71 | 1.67 |
| N_{MV} | above the front bogie | 1.98 | 1.84 | 1.75 | 1.70 | 1.66 |
| | above the rear bogie | 2.13 | 2.01 | 1.93 | 1.87 | 1.83 |

8. Conclusions

This paper deals with the influences of the carbody vertical flexibility of a passenger vehicle on the ride comfort evaluated by the comfort index calculated in three reference points of the carbody – at the centre and above the bogies. To this purpose, a model of the vehicle including a “flexible carbody” model has been used, as well as the elements contributing to the excitation of the symmetrical vertical bending mode of the carbody. It is about the fact that the model of the secondary suspension has included the vertical and pitch stiffness and the stiffness of the longitudinal traction system between the carbody and the bogie.

The results of the numerical simulations confirm the significance of the vertical symmetrical bending of the carbody on the dynamic response of the vehicle, mainly at high velocities and the fact that the ride comfort is greatly affected should the frequency of this vibration mode is lower than 10 Hz. An improvement of the ride comfort can be obtained via an appropriate selection of the longitudinal stiffness of the longitudinal traction system between the carbody and the bogie. Similarly, the value of the comfort index is influenced by the suspension damping ratio. Irrespective of the carbody bending frequency, it has been shown that there is a value of the secondary suspension damping that minimizes the comfort index in any of the carbody reference points. On the other hand, the ride comfort improves at a higher value of the primary suspension damping.

Acknowledgements

This work has been funded by University Politehnica of Bucharest, through the “Excellence Research Grants” Program, UPB – GEX – 2016. Research project title: *Research on developing mechanical and numerical models for the virtual evaluation of the dynamic performances in the railway vehicles* (in Romanian). Contract number: 48/26.09.2016.

References

- [1] M. Dumitriu and I. Sebeşan. The quality of railway vehicles. MatrixRom, Bucharest, 2016. (in Romanian).
- [2] J. Zhou, R. Goodall, L. Ren, and H. Zhang. Influences of car body vertical flexibility on ride quality of passenger railway vehicles. *Proceedings of the Institution of Mechanical Engineers, Part F: Journal of Rail and Rapid Transit*, 223(5):461–471, 2009. doi: 10.1243/09544097JRRT272.
- [3] G. Diana, F. Cheli, A. Collina, R. Corradi, and S. Melzi. The development of a numerical model for railway vehicles comfort assessment through comparison with experimental measurements. *Vehicle System Dynamics*, 38(3):165–183, 2002. doi: 10.1076/vesd.38.3.165.8287.
- [4] F. Cheli and R. Corradi. On rail vehicle vibrations induced by track unevenness: Analysis of the excitation mechanism. *Journal of Sound and Vibration*, 330(15):3744–3765, 2011. doi: 10.1016/j.jsv.2011.02.025.
- [5] D. Gong, J. Zhou, and W. Sun. On the resonant vibration of a flexible railway car body and its suppression with a dynamic vibration absorber. *Journal of Vibration and Control*, 19(5):649–657, 2013. doi: 10.1177/1077546312437435.
- [6] M. Dumitriu. Analysis of the dynamic response in the railway vehicles to the track vertical irregularities. Part II: The numerical analysis. *Journal of Engineering Science and Technology Review*, 8(4):32–39, 2015.
- [7] P. Carlbom. *Carbody and Passengers in Rail Vehicle Dynamics*. Ph.D. Thesis, KTH, Vehicle Engineering, Stockholm, Sweden, 2000. NR 20140805.
- [8] T. Tomioka, T. Takigami, and Y. Suzuki. Numerical analysis of three-dimensional flexural vibration of railway vehicle car body. *Vehicle System Dynamics*, 44(sup1):272–285, 2006. doi: 10.1080/00423110600871301.
- [9] M. Dumitriu. On the critical points of vertical vibration in a railway vehicle. *Archive of Mechanical Engineering*, 61(4):609–625, 2014. doi: 10.2478/meceng-2014-0035.
- [10] ENV 12299: Railway applications ride comfort for passengers measurement and evaluation, 1997.
- [11] UIC 513 R: Guidelines for evaluating passenger comfort in relation to vibration in railway vehicle. International Union of Railways, 1994.
- [12] S. Bruni, J. Vinolas, M. Berg, O. Polach, and S. Stichel. Modelling of suspension components in a rail vehicle dynamics context. *Vehicle System Dynamics*, 49(7):1021–1072, 2011. doi: 10.1080/00423114.2011.586430.
- [13] H. Ye, J. Zeng, Q. Wang, and X. Han. Study on carbody flexible vibration considering layout of underneath equipment and doors. In *Proceedings of 4th International Conference on Sensors, Measurement and Intelligent Materials (ICSMIM 2015)*, pages 1177–1183, Shenzhen, China, 27-28 Dec. 2015. Atlantis Press, 2016. doi : 10.2991/icsmim-15.2016.217.
- [14] K. Wang, H. Xia, M. Xu, and W. Guo. Dynamic analysis of train-bridge interaction system with flexible car-body. *Journal of Mechanical Science and Technology*, 29(9):3571–3580, 2015. doi: 10.1007/s12206-015-0801-y.
- [15] C 116: Interaction between vehicles and track, RP 1, Power spectral density of track irregularities, Part 1: Definitions, conventions and available data, 1971.
- [16] I. Sebeşan and T. Mazilu. Vibrations of the railway vehicles. MatrixRom, Bucharest, 2010. (in Romanian).
- [17] J. Zhou and S. Wenjing. Analysis on geometric filtering phenomenon and flexible car body resonant, vibration of railway vehicles. *Journal of Tongji University, Natural Science*, 37(12):1653–1657, 2009.

- [18] D. Gong, Y.J. Gu, and J.S. Zhou. Study on geometry filtering phenomenon and flexible car body resonant vibration of articulated trains. In *Advanced Materials Researches, Engineering and Manufacturing Technologies in Industry*, volume 787 of *Advanced Materials Research*, pages 542–547. Trans Tech Publications, Nov. 2013. doi: 10.4028/www.scientific.net/AMR.787.542.
- [19] F. Cheli and R. Corradi. On rail vehicle vibrations induced by track unevenness: Analysis of the excitation mechanism. *Journal of Sound and Vibration*, 330(15):3744–3765, 2011. doi: 10.1016/j.jsv.2011.02.025.
- [20] M. Dumitriu. Geometric filtering effect of vertical vibrations of railway vehicles. *Analele Universității “Eftimie Murgu” Resița*, (1):48–61, 2012.
- [21] M. Dumitriu. Considerations on the geometric filtering effect of the bounce and pitch movements in railway vehicles. *Annals of the Faculty of Engineering Hunedoara*, 12(3):155–164, 2014.